

1 **Article Title:** Navigating north: how body mass and winds shape avian flight
2 behaviors across a North American migratory flyway

3 **Authors:** Kyle G. Horton^{1,2,3,5*}, Benjamin M. Van Doren⁴, Frank A. La Sorte⁵, Daniel
4 Fink⁵, Daniel Sheldon^{6,7}, Andrew Farnsworth⁵, and Jeffrey F. Kelly^{1,2}

5 **Email addresses:**

6 KGH: hortonkg@ou.edu, BMVD: benjamin.vandoren@zoo.ox.ac.uk, FAL:
7 fal42@cornell.edu, DF: daniel.fink@cornell.edu, DS: sheldon@cs.umass.edu, AF:
8 af27@cornell.edu, JFK: jkelly@ou.edu

9 **Affiliations:**

10 ¹Department of Biology, University of Oklahoma, Norman, Oklahoma, USA.

11 ²Oklahoma Biological Survey, University of Oklahoma, Norman, Oklahoma, USA.

12 ³Advanced Radar Research Center, University of Oklahoma, Norman, Oklahoma,
13 USA.

14 ⁴Edward Grey Institute, Department of Zoology, University of Oxford, Oxford, OX1
15 3PS, UK

16 ⁵Cornell Lab of Ornithology, Cornell University, Ithaca, New York, USA.

17 ⁶College of Information and Computer Sciences, University of Massachusetts,
18 Amherst, MA, USA

19 ⁷Department of Computer Science, Mount Holyoke College, South Hadley, MA, USA

20 ***Corresponding author:** [Kyle G. Horton](mailto:kyle.g.horton@ou.edu), University of Oklahoma, Department of
21 Biology, 730 Van Vleet Oval, Norman, Oklahoma, USA. Phone: (716) 279- 5710.
22 Email: hortonkg@ou.edu

23 **Short running title:** Body size and winds shaping avian flight behaviors

24 **Keywords:** citizen science, eBird, flight biology, macroecology, seasonal bird
25 migration, radar, remote sensing, wind drift
26 **Article type:** Letter
27 **Number of words:**
28 Abstract: 146
29 Main body: 5074
30 **Number of references:** 91
31 **Number of figures:** 6
32 **Number of tables:** 0
33 **Authors' contributions.** KGH, BVD, AF, and JFK worked to conceive and design this
34 study. KGH processed radar and wind data, generated figures, and drafted the
35 manuscript. BVD and KGH conducted statistical analyses. DF designed and
36 implemented the species distribution models, and FAL and DF designed the analysis
37 of the model products. BVD designed species trajectory analyses and flight behavior
38 models. DS designed radar-processing algorithms. All the authors have provided
39 editorial advice, approved the final version of this manuscript, and agree to be
40 accountable for all aspects of the work.
41 **Data Accessibility** Raw data will be made accessible on Dryad if the article is
42 accepted for publication.

43 **Abstract**

44 The migratory patterns of birds have been the focus of ecologists for millennia.
45 What behavioral traits underlie these remarkably consistent movements?
46 Addressing this question is central to advancing our understanding of migratory
47 flight strategies and requires the integration of information across levels of
48 biological organization, e.g. species to communities. Here, we combine species-
49 specific observations from the eBird citizen-science database with observations
50 aggregated from weather surveillance radars during spring migration in central
51 North America. Our results confirm a core prediction of migration theory at an
52 unprecedented national scale: body mass predicts variation in flight strategies
53 across latitudes, with larger-bodied species flying faster and compensating more for
54 wind drift. We also find evidence that migrants traveling northward earlier in the
55 spring increasingly compensate for wind drift at higher latitudes. This integration of
56 information across biological scales provides new insight into patterns and
57 determinants of broad-scale flight strategies of migratory birds.

MAIN TEXT:

(a) Introduction

Migration is one dimension of a global, ecological system response to the seasonality of Earth's productivity (Mueller & Fagan 2008; Baguette *et al.* 2013; Way & Montgomery 2015). Migration is ubiquitous among a diverse array of taxonomic groups, varying in nearly as many ways as the taxa engaging in these movements. Such variation may have significant implications for individuals in terms of fitness as well as for populations of individuals and the environments in which they occur (e.g. Bonte *et al.* 2012; La Sorte *et al.* 2014a). Migratory behavior varies among species based on mode, speed, duration, body mass, and scale—all of which are dictated by the physical and natural environment in which it occurs. In turn, migration affects the structure and function of the ecosystems that these species occupy across the annual cycle (Fridley 2001; Bauer & Hoyer 2014; Chapman *et al.* 2015b; Hennen *et al.* 2017). Of all the taxonomic groups that display migratory behavior, birds have received the greatest attention (Newton 2008). During migratory journeys, which may last weeks or months, birds must decide when to fly, and once in flight make decisions on the direction, speed, and duration of flight (e.g. Votier 2018).

Varying wind conditions present major challenges for aerial navigators, and understanding birds' context-dependent responses to winds aloft is fundamental to understanding avian navigation. Successful movements depend strongly on these behaviors, which directly affect survivorship and fitness. With the exception of

precipitation, wind is the most important meteorological factor determining migratory behavior (Richardson 1978, 1990). Tailwinds create the optimal migration conditions (Alerstam 1979; Åkesson & Hedenström 2000), but extensive geographic variation in the strength and direction of prevailing winds may dictate migration departure during locally suboptimal conditions (Liechti 2006; Sjöberg *et al.* 2015; Horton *et al.* 2016b). Migrants must contend with getting blown off course, making constant en route adjustments that may incur proximate (e.g., energetic costs) or ultimate consequences (e.g., death or failure to breed). Documenting the relationship among migratory behaviors, traits of migrants, and wind conditions at the scale of an entire migration system is a grand challenge in migration research (e.g., Klaassen *et al.* 2010; Lanzone *et al.* 2012; Sergio *et al.* 2014; Wikelski *et al.* 2015; Flack *et al.* 2016; Åkesson *et al.* 2016; Vansteelant *et al.* 2017b, a).

The ecological systems migrants inhabit are inherently complex and are not mechanistic combinations of their constituent parts (individuals; Holling 1973). Models of optimal migration behavior have made significant progress in revealing the factors constraining broad-scale seasonal movements (Erni *et al.* 2002, 2003, 2005; Vrugt *et al.* 2007; Kranstauber *et al.* 2015). However, more efficient approaches are still needed to amass and analyze data that characterize rich emergent behavioral characteristics of migration systems, which remains a principal challenge (Shiple *et al.* 2017). Understanding global bird movements, and in particular, their adaptations to predictable patterns in atmospheric circulation is an area of active research (La Sorte *et al.* 2014b; Chapman *et al.* 2015a; Kranstauber

et al. 2015). An alternative to an individual-based strategy for studying day-to-day variation in migratory behavior is an approach where the migration system's aggregate properties themselves are studied (e.g., La Sorte *et al.* 2013). By measuring these properties directly, rather than attempting to reconstruct them from individual constituents, we can efficiently quantify dominant long-term and large scale system-level behaviors. To this end, we use a data-intensive approach to examine this interaction. Specifically, we address two long-standing ecological questions: How do migrant birds adjust their flight strategies in response to predictable large scale patterns in atmospheric conditions; and what is the role of a dominant life history trait, body mass, in this response?

Weather surveillance radar (WSR) can measure the emergent properties of avian migration systems, capturing the aggregate behaviors of millions of individual migrants moving through the atmosphere (Kelly & Horton 2016). Although WSR can detect these movements at continental extents, they cannot resolve species identities (Gauthreaux & Belser 1998), a feature that has historically imposed stark limitations on WSR-based inferences (Kelly & Horton 2016). However, the rapid growth and accessibility of citizen science data, specifically the eBird enterprise (Sullivan *et al.* 2014), have transformed our understanding of avian migration at the population scale using a species-level perspective (Silvertown 2009; Hochachka *et al.* 2012; Hurlbert & Liang 2012; La Sorte *et al.* 2013, 2016; La Sorte & Fink 2017). Furthermore, species-level information from eBird can be used to enhance the aggregate-level information available from WSR (La Sorte *et al.* 2015a, b). Although

eBird observations are made primarily during diurnal periods, and do not directly characterize nocturnal movements, the merger of eBird data with WSR-derived nocturnal estimates of migratory birds aloft has the potential to reveal the translation from species-specific properties to system-based properties. For instance, we can address how the aggregate migrant body mass (eBird) scale with the aggregate measures of migrant airspeed (radar). This merger is a natural advancement toward the growth of a macroecological sensing network for studying the broad-scale patterns and determinants of avian migration systems.

Theoretical predictions of the behavior of migrating birds abound (Pennycuick 1969; Alerstam 1979; Alerstam & Hedenström 1998), and recent system-level investigations of stopover behavior have mapped migration trajectories (La Sorte *et al.* 2013, 2016). The influence of prevailing winds on birds' flight strategies are well known in the context of optimal migratory movements (Liechti 2006, Chapman *et al.* 2011, Horton *et al.* 2016a); however, whether migrants need to routinely select for opposing winds in a context dependent manner remains unresolved, specifically with respect to proximity to their end destination. For this investigation, the prediction that body mass, as a driver of life history and energetics (e.g., Nagy 1987), ought to drive variable wind compensation behavior among migrants is a key to investigating context-dependent behaviors. Indeed, at the scale of individuals there is robust evidence of body mass driving flight strategies of migrants (Alerstam *et al.* 2007). We investigate these relationships at the scale of the migration flyway, which has not been done previously.

150

151 Migration theory predicts that migrants should tolerate wind drift near the origin of
152 their migratory route and increase the degree to which they compensate for wind
153 drift as they near their ultimate destination (Alerstam 1979; Liechti 2006).

154 Additionally, morphological constraints (e.g. body mass and its impact on maximum
155 flight speed) may limit species abilities to fully compensate, with large-bodied faster
156 flying migrants showing greater compensatory abilities. The central portion of
157 North American offers an ideal locality to test this hypothesis. This region extends
158 upwards of ~2500 km from subtropical habitats bordering the Gulf of Mexico,
159 across the grasslands of the Great Plains, and extending into the boreal forest near
160 the Canadian border. This region is only minimally influenced by major ecological
161 barriers (e.g., mountains, lakes, or deserts) or leading lines (i.e., coastlines or rivers),
162 that may otherwise affect flight strategies (Horton *et al.* 2016c). Here, we use data
163 from 20 WSR stations and bird observations from eBird (Sullivan *et al.* 2014) to test
164 our optimal flight strategy predictions. Additionally, we examine how the quality of
165 our predictions are affected by two traits that dictate in-flight migratory behavior:
166 body mass, an important morphological trait, and migration destination, an
167 important natural history trait.

168 **(b) Materials and methods**

170 **Weather surveillance radar**

171 We processed unfiltered (i.e., level-II) **Weather Surveillance Radar 1988 Doppler**
172 (WSR-88D) data from 20 radar stations covering a large portion of the central USA

from spring 2013 to spring 2015 (21.6° of latitude; Fig. 1) (Crum & Albery 1993). To investigate spring behaviors, we acquired radar data from NOAA's National Centers for Environmental Information (<https://www.ncdc.noaa.gov>) for the period 1 March to 31 May of each year. The National Weather Service (NWS) within the National Oceanic and Atmospheric Administration (NOAA) operates nineteen of these radars and the Department of Defense (DOD) operates one (KGRK). Every 5 to 10 minutes the radars make a series of sequential elevation observations (e.g., 0.5° above horizontal, 1.5°, ... 19.5°), scanning the airspace from 0 to 359° degrees in azimuth at each elevation. The volume coverage pattern (i.e., airspace sampling routine) is tailored to the atmospheric conditions, and for this reason sampling update times can vary.

We retained data between evening and morning civil twilight (i.e., when the sun angle was at least 6° below the horizon) and discarded any aerial samples containing precipitation, which obscures bird movements. Because the number of radar sweeps (1,101,618 sweeps) prevented complete manual screening, we used a two-stage approach to remove weather contamination: First, we removed volume coverage patterns in which 70% of the low elevation (~0.5°) sweep volumes had correlation coefficient (a polarimetric radar variable) values greater than 0.90 or 70% of the sampling volumes had reflectivity measures greater than 35 dBZ (Stepanian *et al.* 2016). Second, we visually screened all remaining sweeps ($n = 250,552$) for weather contamination. Examination of a subset of images following the first automated step (KMVX 2013, $n = 11,543$) revealed that automated filtering

by correlation coefficient and reflectivity returned a 2.7% false negative rate (203 of 7,582). We deemed the false positive rate too high for our biological application (573 of 3,961; 14.5%), mandating the need for manual inspection (step two) (see Fig. S1 for illustrated workflow). This two-stage process resulted in 231,241 sweeps containing weather-free data, which we retained for subsequent stages of filtering and analysis (20.9 % of the total available sweeps).

We used the WSRLIB package (Sheldon 2015) to determine migrant track (flight direction with respect to the ground) and heading (orientation of body axis) from radial velocity and correlation coefficient (ρ_{HV}), respectively, from 55 to 1995 m above ground level (a.g.l.) following Browning & Wexler (1968) and Stepanian & Horton (2015). When necessary, radial velocity measures were dealiased following Sheldon *et al.* (2013). To limit insect contamination, we excluded velocity azimuth displays (a computation of the mean Doppler velocity to derive migrant track and groundspeed) with RMSE (root mean squared error) less than one, and we removed samples with RMSE greater than five to limit poor fits (Dokter *et al.* 2011; Horton *et al.* 2016a). We restricted polarimetric azimuth displays (a computation of the correlation coefficient, ρ_{HV} , to derive heading) to fits with greater than 15% of the variance explained (when fitting ρ_{HV} to a sinusoid) and an average standard deviation in heading direction that was less than 20° (Stepanian & Horton 2015; Horton *et al.* 2016c). Profiles of track and heading were weighted by log-scaled reflectivity (a measure that scales with biological density), constructed from the lowest elevation sweeps, (0.5-4.5°) from 5 to 37.5 km (Farnsworth *et al.* 2015).

For statistical weighting of aerial movements, we calculated the large-scale (20 to 125 km) intensity of migratory movements for all biologically classified sweeps from the lowest elevation sweeps ($\sim 0.5^\circ$) of reflectivity. We calculated intensity (i.e., phenology indices) and directional data from the lowest sweep because it provides a large-scale perspective of migratory behaviors, and we constructed vertical profiles of reflectivity at closer ranges and higher elevation scales because they allow a better sampling of the altitudinal distribution of birds (Buler & Diehl 2009). We summarized radar measures to tenths of the night (i.e., deciles) to avoid sampling changes caused by the duration of the night. We only used data from individual radars on nights where two or more radars acquired usable samples (e.g., those that were dominated by biology) through the night and five or more deciles of the night were sampled at the individual radar. Overall, we retained 106,772 sweeps (9.7 % of the total available sweeps) across 238 unique sampling nights (17,080 unique deciles, see Fig. S2) from three spring migratory seasons.

Winds Aloft

We quantified wind direction and variance aloft with the radar sampling range (5-37.5km) using the North American Regional Reanalysis (NARR) data set (Mesinger *et al.* 2006). NARR models zonal and meridional wind components every three hours at 25-hPa increments at a gridded 32-km spatial resolution. To characterize general nocturnal wind patterns, regardless of migratory activity and precipitation conditions, we extracted the 03:00 UTC wind speeds and directions from measures

between typical avian flight height ranges, 350 to 650 meters above ground level (875-975 hPa)(La Sorte *et al.* 2015a; Horton *et al.* 2016b). We used 03:00 UTC because it mostly closely coincides with peak migration timing (Zehnder *et al.* 2001; Farnsworth *et al.* 2015; Horton *et al.* 2015). We weighted the prevailing directions by wind speed. All dates between 1 March and 31 May from 2013 to 2015 were used to characterize average wind patterns.

For linking biological measures with wind speeds and directions, we aligned the nearest radar measures by time and height above ground level (55 to 1995 m). We weighted the vertical structure of wind speed and direction by vertical profiles of reflectivity. In addition to determining the dominant wind regimes and winds used by migrants, we used winds aloft to calculate migrant airspeed (powered flight speed). Knowing groundspeed, wind direction, and wind speed, we calculated migrant airspeeds through vector subtraction. As an additional step to limit insect contamination, we eliminated individual height bins (100 m resolution) with airspeeds less than 5 m s^{-1} (Larkin 1991; Gauthreaux & Belser 1998, ~28.5% of altitudinal samples). Following the condensation of the data to deciles, we observed the distribution of mean airspeed measures to be long-tailed (skewed-right), and for this reason we eliminated samples with airspeeds greater than 30 m s^{-1} ($n = 67$ deciles, ~0.99 quantile), a threshold at the upper range of a typical migrant (Alerstam *et al.* 2007).

eBird

We used spatio-temporal exploratory models (STEM) developed by Fink *et al.* (2010) to estimate weekly probability of occurrence of nocturnally migrating bird species using bird observations from the eBird database Sullivan *et al.* (2014) compiled during the period 2004 to 2011. Because the STEM procedure is computationally very intensive, directly matching the temporal range of the radar data with the STEM estimates was not feasible. In addition, the 2004-2011 implementation is currently the most comprehensive where the largest proportion of the North America avifauna was analyzed. We observed comparable wind directions and speeds across the two time periods, and thus do not feel timing differences are of concern (Fig. S3). From 446 species, we classified 157 as nocturnal migrants having probabilities of occurrence that were greater than 0 in our sampling area after applying the thresholding procedure describe below (see Table S1). STEM models use underlying landscape (landcover, elevation), temporal (year, day of year, time of day), location (latitude and longitude), and effort (duration, distance, number of observers) information to produce probabilities of species occurrence. For the STEM analysis, eBird data were limited to stationary and traveling counts (≤ 8.1 km) with local start times between 05:00 and 20:00 and counts that were less than 3 hours in duration. STEM uses an ensemble of randomized overlapping local models, which are each applied across a restricted geographical and temporal extent (Fink *et al.* 2010), to discern associations between observed patterns of bird occurrence (eBird data) and local land-cover characteristics (Fry *et al.* 2011). The assembly of these models are used to make spatial and temporal predictions for the distribution of each species throughout the

year based on local land-cover characteristics. These estimates represent the probability of observing a species by an eBird participant that searches from 07:00 to 08:00 while traveling 1 km. See Fink et al. (2010) for additional details on the STEM procedure.

The weekly estimates of probability of occurrence for each of the 157 species were rendered at 130,751 points at a density of *ca.* 15 per 30 × 30 km within the contiguous USA using a geographically stratified random design (SRD) (see Fig. S4). We used previously described methods to remove SRD points that contained very low probabilities of occurrence (La Sorte *et al.* 2014b). Specifically, we converted weekly estimates of probability of occurrence to zero that were less than or equal to the 80th percentile of the non-zero occurrence probabilities for that week, and if the 80th percentile was <0.0175, which defined our minimum probability threshold, the probability threshold was set to 0.0175.

We then calculated the mean probability of occurrence for species at each WSR station during each week using the SRD points that occurred within a 125-km radius of each WSR station (see Fig. S4). We defined presence/absence for the species richness calculations if the mean probability of occurrence of a species at a WSR station was greater than zero. We derived body mass estimates for each of the 157 species from Dunning (2008); sex- and subspecies-specific masses were averaged following La Sorte et al. (2015). To calculate average body mass within the radar coverage area we weighted body masses by the underlying species STEM

occurrence.

We used NatureServe breeding range map polygons (Ridgely *et al.* 2007) to estimate the direction of movement and distance between centers of species' distributions and radar locations for the 157 species. We used the angles to predict the population-level direction of movement of species reflected in the radar measures. For each radar station and each species, we calculated the angle from the station to the center of the breeding range following formulae by Snyder (1987). We only retained distances from angles $< 90^\circ$ and $> 270^\circ$ because these species should be making progress northward towards their breeding range. For each radar station and week, we calculated the mean angle of all species (Fig. S5 and S6), weighted by the proportional occurrence from STEM models. The proportional occurrence was calculated weekly, by dividing the square root of the species-specific STEM model occurrences within the radar domain by the square root of the weekly summed total occurrence (for all species) within the radar domain. We used the square-root transformation to reduce the range of weights, preventing conspicuous species from dominating the weighting procedure. The resulting weighted average of trajectory angles, weighted by proportional occurrence, was the eBird-derived predicted direction of movement for a given radar station and time point.

Statistical analysis

We based our approach on the methods of Green & Alerstam (2002) to determine the degree of compensation for wind drift and radar-derived preferred direction of

movement (Chapman *et al.* 2011; Kemp *et al.* 2012). In brief, we used a mixed model to regress radar measures of track on the difference between track and heading (α) (Green & Alerstam 2002; Horton *et al.* 2016c; Van Doren *et al.* 2016). This model is used to derive two important metrics describing migrant flight strategy: (1) slope of α versus track, a measure of the propensity of drift (0 = complete compensation for wind drift; 1 = no compensation, or total drift), and (2) the y-intercept of this regression, the direction at which birds align themselves downwind, which is a measure of the preferred direction of movement.

To test for effects of latitude and body mass on flight strategies, we constructed a linear mixed-effects model with α , average body mass, latitude, day of year, and all possible interactions as fixed predictors. To simplify the model, we removed the four-way interaction term, which was not statistically significant (see Table S2 and S3 for model details). We standardized (mean=0, sd=1) body mass after subtracting 30 g and rescaled latitudes so that the mean latitude was zero. We also standardized day of year (mean=0, sd=1). Therefore, the intercepts of the model would be at a body mass of 30 g, the mass of a medium-sized migratory songbird, and the mean latitude and mean time of season. Random intercept terms were station, station x year, date, and station x date. We included one random slope term, of α varying on station. We weighted our analysis by scaled radar reflectivity. We used body mass to differentiate how coarse taxonomic shifts influence flight behavior. Body mass distributions showed general separation by order (Fig. S7) and by timing of movement (Fig. S8). For model predictions, we display the 20th, 40th, 60th, and 80th

percentile of the average system-based body masses; 40, 60, 80, and 140 grams.

We visualized uncertainty in model predictions by bootstrapping 95% confidence intervals of key parameters of interest. Bootstrapping is recommended by the authors of *lme4* for determining uncertainty in mixed-model predictions. We also elected to perform bootstrapping because the residual distribution was long-tailed, which may bias conventional *p*-values.

All statistical analyses were conducted in R version 3.3.3 (R Core Team 2017), and linear mixed models implemented using the *lme4*. All summary statistics are reported with 95% confidence intervals unless otherwise stated.

(c) Results

Weather surveillance radar

Migratory activity increased during the second week of April and peaked between 30 April and 20 May. Date of peak reflectivity was correlated with latitude ($r = 0.89$, $t_{18} = 8.02$, $p < 0.001$), showing a 10-day difference between latitudinal extremes (KBRO and KVMX) (Fig. 2a). Overall, track direction averaged slightly more eastward-facing ($3.20 \pm 5.66^\circ$) than heading ($359.13 \pm 6.78^\circ$) (Fig. 1). Flight directions changed systematically with latitude, with tracks shifting $2.30 \pm 0.48^\circ$ ($p < 0.001$) and heading $3.23 \pm 0.61^\circ$ ($p < 0.001$) westward with each increase in degree latitude. Across all sites, airspeeds by station averaged 10.89 ± 1.26 m/s (lowest, KHGX,

8.42±1.26 m/s; highest, KABR, 13.34±1.29 m/s). Through the season, airspeeds declined for 19 of 20 sites, most sharply for high latitude sites (Fig. 3a), and tended to average higher with increasing latitude (slope = 0.18±0.06 m/s, $R^2=0.59$, $df=18$, $p<0.001$). Overall, we saw a significant decline in airspeed through the season (slope = 0.026±0.0023 m/s, $p<0.001$).

eBird

Species richness generally increased throughout the season, rising more rapidly with increasing latitude (Fig. 2b). The three most speciose and highest occurring orders were Passeriformes ($n=115$), Charadriiformes ($n=19$), and Anseriformes ($n=14$) (Fig. S9, Fig. S10). Average body mass of species detected at the most northern WSR stations (e.g., KMOV, KDLH; Fig. 2c) increased early in the season and then decreased for the remainder of the season. Otherwise, there was a general decline in body mass through the season, with a slight increase toward the end May. This peak in migrant body size was driven by shifts in species composition (Fig. S9, Fig. S10); large-bodied Anseriformes dominated early season occurrence patterns but gave way to small-bodied Passeriformes later in the season.

Combining radar and eBird

We examine three sets of behavioral measures: 1.) airspeed (radar) and body mass (eBird), 2.) preferred (radar) and predicted (eBird) directions of movement, and 3.) how these factors influence how migrants cope with wind drift across a latitudinal gradient.

Average body mass within the radar coverage estimated from eBird STEM models explained a significant amount of variation in average airspeed (slope = 0.13 ± 0.06 , $R^2=0.54$, $df = 18$, $p<0.001$; Fig. 3b). Like radar-derived preferred directions of movement (slope = $2.67 \pm 0.75^\circ$, $R^2=0.73$, $df=18$, $p<0.001$, Fig. 2), eBird-derived predicted directions of movement shifted westward with increasing latitude (slope = $2.36 \pm 0.71^\circ$, $R^2=0.70$, $df=18$, $p<0.001$) (Fig. 4). Predicted direction of movement from eBird explained 84% of the variation in radar-derived preferred direction of movement estimates ($df = 18$, $p<0.001$; Fig. 4).

Body mass, latitude, and date all significantly affected flight direction and drift strategy (Table S3). Birds generally compensated for drift to an increasing extent as latitude increased (Fig. 5). This latitudinal contrast was greatest among smaller-bodied birds and earlier in the season; the effect largely disappeared by late May. In general, larger bodied birds compensated more than smaller bodied birds. Time of season showed the strongest influence on flight strategy: birds of all body masses and across all latitudes compensated less as the season progressed. The preferred direction of migration shifted westward with increasing latitude (Fig 1.), especially later in the season (Fig. 6), and shifted eastward with increasing body mass (Fig. 6), especially early in the season.

Wind

Seasonal wind direction originated increasingly from the west at higher latitudes

(slope= $7.37 \pm 2.07^\circ$, $p < 0.001$, $R^2 = 0.74$) and became more variable in direction at higher latitudes (slope of variance= $3.19 \pm 0.93^\circ$, $p < 0.001$, $R^2 = 0.73$). Similarly, although less dramatically, wind directions weighted by migratory activity showed a westerly shift at higher latitudes (slope= $1.38 \pm 0.80^\circ$, $p < 0.01$, $R^2 = 0.38$). Winds used by migrants were more variable in direction with increasing latitude (slope= $2.36 \pm 0.68^\circ$, $p < 0.001$, $R^2 = 0.72$).

(d) Discussion

We show through a process of data integration how the in-flight strategies of the migratory system change through the season and across a broad latitudinal gradient. Our results give system-level support for our optimal migration hypotheses. Across 20 WSR stations, we found evidence that nocturnal migrants increasingly compensated for wind drift as they progressed northward through the center of North America, especially early in the spring. Additionally, faster-flying, larger-bodied migrants compensated more for wind drift, regardless of latitude. Our findings support our prediction that migrants compensate more for wind drift at higher latitudes during spring migration, with smaller-sized songbirds showing the strongest shifts. The multitude of significant interactions in our model highlight the complexity of these flight strategy patterns and their dependence on time of season and species composition.

The emergent flight strategies of migrating birds are complex integrations of multiple biotic and abiotic factors. A primary component is maximum airspeed,

which defines a species' ability to compensate for wind drift (Alerstam 1979; Green & Alerstam 2002). Large-bodied species, which have the morphological capacity to fly faster, have an increased capability to successfully counter wind drift (Pennycuick 1969; Alerstam & Hedenström 1998; Alerstam *et al.* 2007; Hedenström 2008). Ground-based eBird derived observations of species composition across our study region shows a seasonal shift from early, large-bodied, fast-flying migrants to late, small-bodied, slow flying migrants. The positive relationship between species body mass estimated from ground-based eBird observations and WSR based estimates of in-flight nocturnal airspeeds is an exciting integration of these two independent data sets. These findings follow predictions from aerodynamic first principles based on individual behavior (Pennycuick 1969; Alerstam 2003). We show a strong correspondence with airspeed-body mass scaling coefficients measured on individually tracked migrants (0.12, Alerstam *et al.* 2007) and at the system-level (0.13, see Fig. 3), giving additional support to our finding that aggregate eBird properties can predict large-scale migratory movements detected by weather surveillance radar. Never has this relationship been detected at a flyway scale for millions of migrating individuals. These findings suggest that body size is a critical trait driving migration biology, and can play an important role in advancing our understanding of broad-scale migration dynamics.

Optimal migration theory predicts that migrants should increase compensation as they approach their end destination to minimize their overall time and energy expenditure (Liechti 2006). We show that smaller-bodied and early-season

migrants made systematic shifts toward greater compensation with increasing latitude. Additionally, preferred directions of movements of nocturnal migrants sensed by WSR shifted to increasingly westerly directions at higher latitudes. We reproduced this pattern with information about species composition from ground-based eBird observations and directions to destination, which suggests that this phenomenon occurs because species with northerly distributions tend to have breeding ranges centered in western North America (Fig. S6). Birds moving towards the northwest must contend increasingly with westerly crosswinds at higher latitudes, compounding the effort needed to compensate for wind drift. Although we cannot confirm whether migrants are increasingly compensating for increasingly unfavorable winds or proximity to their breeding destination, our assessment shows a system-wide behavioral trend in the propensity of drift.

We recognize an important caveat here, that it remains difficult to assess the influence of pseudodrift in our findings. The non-uniformity in preferred flight directions among different species or populations and their choice to fly under different wind conditions can manifest in the appearance of enhanced levels of drift (i.e., pseudodrift) (Evans 1966; Nisbet & Drury 1967; Alerstam 1978). Our analysis was designed to minimize the effect of pseudodrift, accounting for inter-night variation in flight direction using random effects and leaving the fixed effects to describe average patterns within the migratory periods. However, without detailed knowledge of the relationship between the probability of departure and wind direction and speed (e.g., Deppe *et al.* 2015), quantifying pseudodrift remains a

principle challenge. The question of the general behavioral mechanisms that enable individual migrants to cope with these unfavorable conditions and ultimately arrive precisely at their destinations remains open.

Species' body size and geographic location and how wind speed and direction vary seasonally along migration flyways are likely the primary factors affecting compensation strategies. Winds aloft, in particular, appear to be an important component determining the seasonal composition of migrants within a flyway (Kranstauber *et al.* 2015). Geographic tendencies in wind speed and direction may shape observed flight behaviors, as well as their phenologies. The low-level nocturnal jet stream of the Great Plains brings strong, southerly winds from the Gulf of Mexico, generally peaking in intensity through the mid-latitudes of the United States (Walters *et al.* 2008). The low-level jet influences spring migratory pathways (La Sorte *et al.* 2014b) and nightly flight behaviors (e.g., flight height selection; Wainwright *et al.* 2016). Additionally, the behavior of the low-level jet, in concert with the polar front and subtropical jet stream, which drive synoptic weather patterns west to east (Archer & Caldeira 2008; Pena-Ortiz *et al.* 2013), helps to explain our findings of winds originating increasingly from the west at higher latitudes, in addition to greater seasonal variation in wind directions at more northerly sites. Our findings carry significance when considering the implications of projected changes in the region's prevailing winds under global warming. The low-level jet in the south is projected to increase in strength (Cook *et al.* 2008), and the prevailing westerlies in the north are projected to decrease in strength (Francis &

Vavrus 2012; Li *et al.* 2012); the former may increase migration speeds, while the latter may diminish the need for compensation (La Sorte & Fink 2016). In total, these changes may enhance flight efficiency during spring migration. It remains to be seen how these behaviors contrast with fall migratory movements, where winds are expected to be less favorable for southbound flights (La Sorte *et al.* 2014b; Wainwright *et al.* 2016).

Characterizing a multi-dimensional biological system like bird migration with observational and remote sensing data highlights the power of ecological analyses in the era of big data (Hampton *et al.* 2013; Schimel & Keller 2015). Citizen scientists can collect direct observations of species on the ground that can be synthesized into state-of-the-art distribution maps. The WSR network in the USA can detect hundreds of millions, if not billions, of migrating birds each year, making it a sensor network with unparalleled potential to study and monitor migration systems. We show that it is possible to integrate these datasets representing models of concurrent species distributions derived from ground-based observations and aerial distributions of nocturnally migrating birds to advance our understanding of the patterns and dynamics of migration systems.

(e) Acknowledgements

We thank Thomas Alerstam, Wesley Hochachka, Cecilia Nilsson, and Michael Patten for comments on earlier drafts of the manuscript. We thank Gil Bohrer and three other anonymous reviewers for their constructive commentary. We would like to

539 thank Steve Kelling and the eBird team for their support, and the many contributors
540 to the eBird database. Funding for this project was provided by the Leon Levy
541 Foundation and the National Science Foundation (DBI-1661329; EF-1340921; IIS-
542 1125098; ABI sustaining: DBI-1356308; ABI innovation: DBI-1661259; computing
543 support from OCI-1053575 and DEB-110008).

(f) Literature Cited:

- Åkesson, S., Bianco, G. & Hedenström, A. (2016). Negotiating an ecological barrier: crossing the Sahara in relation to winds by common swifts. *Phil Trans R Soc B*, 371, 20150393.
- Akesson, S. & Hendenström, A. (2000). Wind selectivity of migratory flight departures in birds. *Behav Ecol Sociobiol*, 47, 140–144.
- Alerstam, T. (1978). A graphical illustration of pseudodrift. *Oikos*, 30, 409–412.
- Alerstam, T. (1979). Wind as selective agent in bird migration. *Ornis Scand.*, 10, 76–93.
- Alerstam, T. (2003). Bird migration speed. In: *Avian Migration* (eds. Berthold, P., Gwinner, E. & Sonnenschein, E.). Springer-Verlag, Berlin, pp. 253–267.
- Alerstam, T. & Hedenström, A. (1998). The development of bird migration theory. *J. Avian Biol.*, 29, 343–369.
- Alerstam, T., Rosén, M., Bäckman, J., Ericson, P.G.P. & Hellgren, O. (2007). Flight speeds among bird species: allometric and phylogenetic effects. *PLOS Biol.*, 5, e197.
- Archer, C.L. & Caldeira, K. (2008). Historical trends in the jet streams. *Geophys. Res. Lett.*, 35, L08803.
- Baguette, M., Blanchet, S., Legrand, D., Stevens, V.M. & Turlure, C. (2013). Individual dispersal, landscape connectivity and ecological networks. *Biol. Rev.*, 88, 310–326.

564 Bauer, S. & Hoyer, B.J. (2014). Migratory Animals Couple Biodiversity and Ecosystem
565 Functioning Worldwide. *Science*, 344, 1242552.

566 Bonte, D., Van Dyck, H., Bullock, J.M., Coulon, A., Delgado, M., Gibbs, M., *et al.*
567 (2012). Costs of dispersal. *Biol. Rev.*, 87, 290–312.

568 Browning, K.A. & Wexler, R. (1968). The determination of kinematic properties of a
569 wind field using Doppler radar. *J. Appl. Meteorol.*, 7, 105–113.

570 Buler, J.J. & Diehl, R.H. (2009). Quantifying bird density during migratory stopover
571 using weather surveillance radar. *IEEE Trans. Geosci. Remote Sens.*, 47, 2741–
572 2751.

573 Chapman, J.W., Klaassen, R.H.G., Drake, V.A., Fossette, S., Hays, G.C., Metcalfe, J.D.,
574 *et al.* (2011). Animal orientation strategies for movement in flows. *Curr. Biol.*,
575 21, R861–R870.

576 Chapman, J.W., Nilsson, C., Lim, K.S., Bäckman, J., Reynolds, D.R. & Alerstam, T.
577 (2015a). Adaptive strategies in nocturnally migrating insects and songbirds:
578 contrasting responses to wind. *J. Anim. Ecol.*, 85, 115–124.

579 Chapman, J.W., Reynolds, D.R. & Wilson, K. (2015b). Long-range seasonal migration in
580 insects: mechanisms, evolutionary drivers and ecological consequences. *Ecol.*
581 *Lett.*, 18, 287–302.

582 Cook, K.H., Vizy, E.K., Launer, Z.S. & Patricola, C.M. (2008). Springtime
 583 intensification of the Great Plains low-level jet and Midwest precipitation in
 584 GCM simulations of the twenty-first century. *J. Clim.*, 21, 6321–6340.

585 Crum, T.D. & Alberty, R.L. (1993). The WSR-88D and the WSR-88D operational
 586 support facility. *Bull. Am. Meteorol. Soc.*, 74, 1669–1687.

587 Deppe, J.L., Ward, M.P., Bolus, R.T., Diehl, R.H., Celis-Murillo, A., Zenzal, T.J., *et al.*
 588 (2015). Fat, weather, and date affect migratory songbirds' departure decisions,
 589 routes, and time it takes to cross the Gulf of Mexico. *Proc. Natl. Acad. Sci.*,
 590 201503381.

591 Dokter, A.M., Liechti, F., Stark, H., Delobbe, L., Tabary, P. & Holleman, I. (2011). Bird
 592 migration flight altitudes studied by a network of operational weather radars. *J. R.*
 593 *Soc. Interface*, 8, 30–43.

594 Dunning, J.B.J. (2008). *CRC handbook of avian body masses, Second Edition*. Boca
 595 Raton, FL.

596 Erni, B., Liechti, F. & Bruderer, B. (2003). How does a first year passerine migrant find
 597 its way? Simulating migration mechanisms and behavioural adaptations. *Oikos*,
 598 103, 333–340.

599 Erni, B., Liechti, F. & Bruderer, B. (2005). The role of wind in passerine autumn
 600 migration between Europe and Africa. *Behav. Ecol.*, 16, 732–740.

601 Erni, B., Liechti, F., Underhill, L.G. & Bruderer, B. (2002). Wind and rain govern the
 602 intensity of nocturnal bird migration in central Europe -- a log-linear regression
 603 analysis. *Ardea*, 90, 155–166.

604 Evans, P.R. (1966). Migration and orientation of passerine night migrants in northeast
 605 England. *J. Zool.*, 150, 319–348.

606 Farnsworth, A., Van Doren, B.M., Hochachka, W.M., Sheldon, D., Winner, K., Irvine, J.,
 607 *et al.* (2015). A characterization of autumn nocturnal migration detected by
 608 weather surveillance radars in the northeastern US. *Ecol. Appl.*

609 Fink, D., Hochachka, W.M., Zuckerberg, B., Winkler, D.W., Shaby, B., Munson, M.A.,
 610 *et al.* (2010). Spatiotemporal exploratory models for broad-scale survey data.
 611 *Ecol. Appl.*, 20, 2131–2147.

612 Flack, A., Fiedler, W., Blas, J., Pokrovsky, I., Kaatz, M., Mitropolsky, M., *et al.* (2016).
 613 Costs of migratory decisions: A comparison across eight white stork populations.
 614 *Sci. Adv.*, 2, e1500931.

615 Francis, J.A. & Vavrus, S.J. (2012). Evidence linking Arctic amplification to extreme
 616 weather in mid-latitudes. *Geophys. Res. Lett.*, 39, L06801.

617 Fridley, J.D. (2001). The influence of species diversity on ecosystem productivity: how,
 618 where, and why? *Oikos*, 93, 514–526.

619 Fry, J., Xian, G., Jin, S., Dewitz, J., Homer, C., Yang, L., *et al.* (2011). Completion of the
620 2006 National Land Cover Database for the conterminous united states.
621 *Photogramm. Eng. Remote Sens.*, 77, 858–864.

622 Gauthreaux, S.A. & Belser, C.G. (1998). Displays of bird movements on the WSR-88D:
623 patterns and quantification. *Weather Forecast.*, 13, 453–464.

624 Green, M. & Alerstam, T. (2002). The problem of estimating wind drift in migrating
625 birds. *J. Theor. Biol.*, 218, 485–496.

626 Hampton, S.E., Strasser, C.A., Tewksbury, J.J., Gram, W.K., Budden, A.E., Batcheller,
627 A.L., *et al.* (2013). Big data and the future of ecology. *Front. Ecol. Environ.*, 11,
628 156–162.

629 Hedenström, A. (2008). Adaptations to migration in birds: behavioural strategies,
630 morphology and scaling effects. *Philos. Trans. R. Soc. B Biol. Sci.*, 363, 287–299.

631 Hessen, D.O., Tombre, I.M., van Geest, G. & Alfsnes, K. (2017). Global change and
632 ecosystem connectivity: How geese link fields of central Europe to eutrophication
633 of Arctic freshwaters. *Ambio*, 46, 40–47.

634 Hochachka, W.M., Fink, D., Hutchinson, R.A., Sheldon, D., Wong, W.-K. & Kelling, S.
635 (2012). Data-intensive science applied to broad-scale citizen science. *Trends Ecol.*
636 *Evol.*, Ecological and evolutionary informatics, 27, 130–137.

637 Holling, C.S. (1973). Resilience and stability of ecological systems. *Annu. Rev. Ecol.*
638 *Syst.*, 4, 1–23.

639 Horton, K.G., Shriver, W.G. & Buler, J.J. (2015). A comparison of traffic estimates of
 640 nocturnal flying animals using radar, thermal imaging, and acoustic recording.
 641 *Ecol. Appl.*, 25, 390–401.

642 Horton, K.G., Van Doren, B.M., Stepanian, P.M., Farnsworth, A. & Kelly, J.F. (2016a).
 643 Seasonal differences in landbird migration strategies. *The Auk*, 133, 761–769.

644 Horton, K.G., Van Doren, B.M., Stepanian, P.M., Farnsworth, A. & Kelly, J.F. (2016b).
 645 Where in the air? Aerial habitat use of nocturnally migrating birds. *Biol. Lett.*, 12,
 646 20160591.

647 Horton, K.G., Van Doren, B.M., Stepanian, P.M., Hochachka, W.M., Farnsworth, A. &
 648 Kelly, J.F. (2016c). Nocturnally migrating songbirds drift when they can and
 649 compensate when they must. *Sci. Rep.*, 6, 21249.

650 Hurlbert, A.H. & Liang, Z. (2012). Spatiotemporal variation in avian migration
 651 phenology: citizen science reveals effects of climate change. *PLoS ONE*, 7,
 652 e31662.

653 Kelly, J.F. & Horton, K.G. (2016). Toward a predictive macrosystems framework for
 654 migration ecology. *Glob. Ecol. Biogeogr.*

655 Kemp, M.U., Shamoun-Baranes, J., Van Loon, E.E., McLaren, J.D., Dokter, A.M. &
 656 Bouten, W. (2012). Quantifying flow-assistance and implications for movement
 657 research. *J. Theor. Biol.*, 308, 56–67.

658 Klaassen, R.H.G., Hake, M., Strandberg, R. & Alerstam, T. (2010). Geographical and
659 temporal flexibility in the response to crosswinds by migrating raptors. *Proc. R.*
660 *Soc. Lond. B Biol. Sci.*, rspb20102106.

661 Kranstauber, B., Weinzierl, R., Wikelski, M. & Safi, K. (2015). Global aerial flyways
662 allow efficient travelling. *Ecol. Lett.*, 18, 1338–1345.

663 La Sorte, F.A. & Fink, D. (2016). Projected changes in prevailing winds for transatlantic
664 migratory birds under global warming. *J. Anim. Ecol.*

665 La Sorte, F.A. & Fink, D. (2017). Migration distance, ecological barriers and en-route
666 variation in the migratory behaviour of terrestrial bird populations. *Glob. Ecol.*
667 *Biogeogr.*, 26, 216–227.

668 La Sorte, F.A., Fink, D., Hochachka, W.M., DeLong, J.P. & Kelling, S. (2013).
669 Population-level scaling of avian migration speed with body size and migration
670 distance for powered fliers. *Ecology*, 94, 1839–1847.

671 La Sorte, F.A., Fink, D., Hochachka, W.M., DeLong, J.P. & Kelling, S. (2014a). Spring
672 phenology of ecological productivity contributes to the use of looped migration
673 strategies by birds. *Proc R Soc B*, 281, 20140984.

674 La Sorte, F.A., Fink, D., Hochachka, W.M., Farnsworth, A., Rodewald, A.D., Rosenberg,
675 K.V., *et al.* (2014b). The role of atmospheric conditions in the seasonal dynamics
676 of North American migration flyways. *J. Biogeogr.*, 41, 1685–1696.

677 La Sorte, F.A., Fink, D., Hochachka, W.M. & Kelling, S. (2016). Convergence of broad-
678 scale migration strategies in terrestrial birds. *Proc. R. Soc. B Biol. Sci.*, 283,
679 20152588.

680 La Sorte, F.A., Hochachka, W.M., Farnsworth, A., Sheldon, D., Doren, B.M.V., Fink, D.,
681 *et al.* (2015a). Seasonal changes in the altitudinal distribution of nocturnally
682 migrating birds during autumn migration. *R. Soc. Open Sci.*, 2, 150347.

683 La Sorte, F.A., Hochachka, W.M., Farnsworth, A., Sheldon, D., Fink, D., Geevarghese,
684 J., *et al.* (2015b). Migration timing and its determinants for nocturnal migratory
685 birds during autumn migration. *J. Anim. Ecol.*, 84, 1202–1212.

686 La Sorte, F.A., Hochachka, W.M., Farnsworth, A., Sheldon, D., Fink, D., Geevarghese,
687 J., *et al.* (2015c). Migration timing and its determinants for nocturnal migratory
688 birds during autumn migration. *J. Anim. Ecol.*, 84, 1202–1212.

689 Lanzone, M.J., Miller, T.A., Turk, P., Brandes, D., Halverson, C., Maisonneuve, C., *et al.*
690 (2012). Flight responses by a migratory soaring raptor to changing meteorological
691 conditions. *Biol. Lett.*, 8, 710–713.

692 Li, W., Li, L., Ting, M. & Liu, Y. (2012). Intensification of Northern Hemisphere
693 subtropical highs in a warming climate. *Nat. Geosci.*, 5, 830–834.

694 Liechti, F. (2006). Birds: blowin' by the wind? *J. Ornithol.*, 147, 202–211.

695 Mesinger, F., DiMego, G., Kalnay, E., Mitchell, K., Shafran, P.C., Ebisuzaki, W., *et al.*
696 (2006). North American Regional Reanalysis. *Bull. Am. Meteorol. Soc.*, 87, 343–
697 360.

698 Mueller, T. & Fagan, W.F. (2008). Search and navigation in dynamic environments –
699 from individual behaviors to population distributions. *Oikos*, 117, 654–664.

700 Nagy, K.A. (1987). Field Metabolic Rate and Food Requirement Scaling in Mammals
701 and Birds. *Ecol. Monogr.*, 57, 112–128.

702 Newton, I. (2008). *The migration ecology of birds*. Academic Press, London, England.

703 Nisbet, I.C.T. & Drury, W.H.J. (1967). Orientation of spring migrants studied by radar.
704 *Bird-Band.*, 38, 173–186.

705 Pena-Ortiz, C., Gallego, D., Ribera, P., Ordonez, P. & Alvarez-Castro, M.D.C. (2013).
706 Observed trends in the global jet stream characteristics during the second half of
707 the 20th century. *J. Geophys. Res. Atmospheres*, 118, 2702–2713.

708 Pennycuik, C.J. (1969). The Mechanics of Bird Migration. *Ibis*, 111, 525–556.

709 R Core Team. (2017). *R: a language and environment for statistical computing*. R
710 Foundation for Statistical Computing. Vienna, Austria.

711 Richardson, W.J. (1978). Timing and amount of bird migration in relation to weather: a
712 review. *Oikos*, 30, 224–272.

713 Richardson, W.J. (1990). Timing of bird migration in relation to weather: updated
714 review. In: *Bird migration*. Springer-Verlag, Berlin, pp. 78–101.

715 Ridgely, R.S., Allnutt, T.F., Brooks, T., McNicol, D.K., Mehlman, D.W., Young, B.E., *et*
716 *al.* (2007). *Digital distribution maps of the birds of the Western Hemisphere*.
717 NatureServe, Arlington, Virginia, USA.

718 Schimel, D. & Keller, M. (2015). Big questions, big science: meeting the challenges of
719 global ecology. *Oecologia*, 177, 925–934.

720 Sergio, F., Tanferna, A., De Stephanis, R., Jiménez, L.L., Blas, J., Tavecchia, G., *et al.*
721 (2014). Individual improvements and selective mortality shape lifelong migratory
722 performance. *Nature*, 515, 410–413.

723 Sheldon, D. (2015). *WSRLIB: MATLAB toolbox for weather surveillance radar*.

724 Sheldon, D., Farnsworth, A., Irvine, J., Van Doren, B., Webb, K., Dietterich, T.G., *et al.*
725 (2013). Approximate Bayesian inference for reconstructing velocities of
726 migrating birds from weather radar. *Assoc. Adv. Artif. Intell.*, 1334–1340.

727 Shipley, J.R., Kelly, J.F. & Frick, W.F. (2017). Toward integrating citizen science and
728 radar data for migrant bird conservation. *Remote Sens. Ecol. Conserv.*, 0.

729 Silvertown, J. (2009). A new dawn for citizen science. *Trends Ecol. Evol.*, 24, 467–471.

730 Sjöberg, S., Alerstam, T., Åkesson, S., Schulz, A., Weidauer, A., Coppack, T., *et al.*
731 (2015). Weather and fuel reserves determine departure and flight decisions in
732 passerines migrating across the Baltic Sea. *Anim. Behav.*, 104, 59–68.

733 Snyder, J.P. (1987). *Map projections: a working manual* (USGS Numbered Series No.
734 1395). Professional Paper. U.S. Government Printing Office, Washington, D.C.

- 735 Stepanian, P.M. & Horton, K.G. (2015). Extracting migrant flight orientation profiles
736 using polarimetric radar. *IEEE Trans. Geosci. Remote Sens.*, 53, 6518–6528.
- 737 Stepanian, P.M., Horton, K.G., Melnikov, V.M., Zrnić, D.S. & Gauthreaux, S.A. (2016).
738 Dual-polarization radar products for biological applications. *Ecosphere*, 7, 1–27.
- 739 Sullivan, B.L., Aycrigg, J.L., Barry, J.H., Bonney, R.E., Bruns, N., Cooper, C.B., *et al.*
740 (2014). The eBird enterprise: an integrated approach to development and
741 application of citizen science. *Biol. Conserv.*, 169, 31–40.
- 742 Van Doren, B.M., Horton, K.G., Stepanian, P.M., Mizrahi, D.S. & Farnsworth, A.
743 (2016). Wind drift explains the reoriented morning flights of songbirds. *Behav.*
744 *Ecol.*, 27, 1122–1131.
- 745 Vansteelant, W.M.G., Kekkonen, J. & Byholm, P. (2017a). Wind conditions and
746 geography shape the first outbound migration of juvenile honey buzzards and
747 their distribution across sub-Saharan Africa. *Proc. R. Soc. B Biol. Sci.*, 284.
- 748 Vansteelant, W.M.G., Shamoun-Baranes, J., van Manen, W., van Diermen, J. & Bouten,
749 W. (2017b). Seasonal detours by soaring migrants shaped by wind regimes along
750 the East Atlantic Flyway. *J. Anim. Ecol.*, 86, 179–191.
- 751 Votier, S. (2018). Bird Migration: Life on the High Seas. *Curr. Biol.*, 28, R21–R23.
- 752 Vrugt, J.A., Van Belle, J. & Bouten, W. (2007). Pareto front analysis of flight time and
753 energy use in long-distance bird migration. *J. Avian Biol.*, 38, 432–442.

754 Wainwright, C.E., Stepanian, P.M. & Horton, K.G. (2016). The role of the US Great
755 Plains low-level jet in nocturnal migrant behavior. *Int. J. Biometeorol.*, 60, 1531–
756 1542.

757 Walters, C.K., Winkler, J.A., Shadbolt, R.P., van Ravensway, J. & Bierly, G.D. (2008). A
758 long-term climatology of southerly and northerly low-level jets for the Central
759 United States. *Ann. Assoc. Am. Geogr.*, 98, 521–552.

760 Way, D.A. & Montgomery, R.A. (2015). Photoperiod constraints on tree phenology,
761 performance and migration in a warming world. *Plant Cell Environ.*, 38, 1725–
762 1736.

763 Wikelski, M., Arriero, E., Gagliardo, A., Holland, R.A., Huttunen, M.J., Juvaste, R., *et al.*
764 (2015). True navigation in migrating gulls requires intact olfactory nerves. *Sci.*
765 *Rep.*, 5, 17061.

766 Zehnder, S., Åkesson, S., Liechti, F. & Bruderer, B. (2001). Nocturnal autumn bird
767 migration at Falsterbo, south Sweden. *J. Avian Biol.*, 32, 239–248.

768

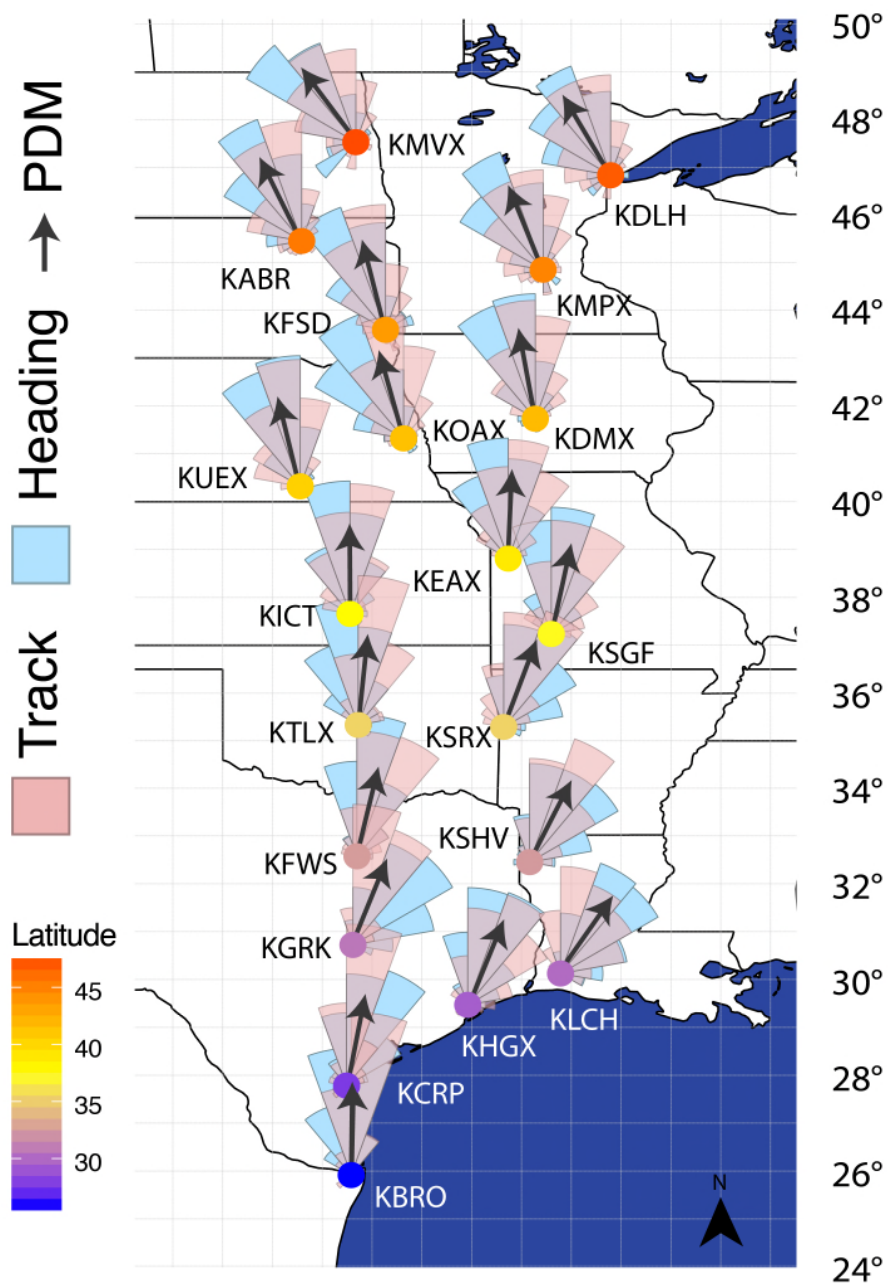


Figure 1:

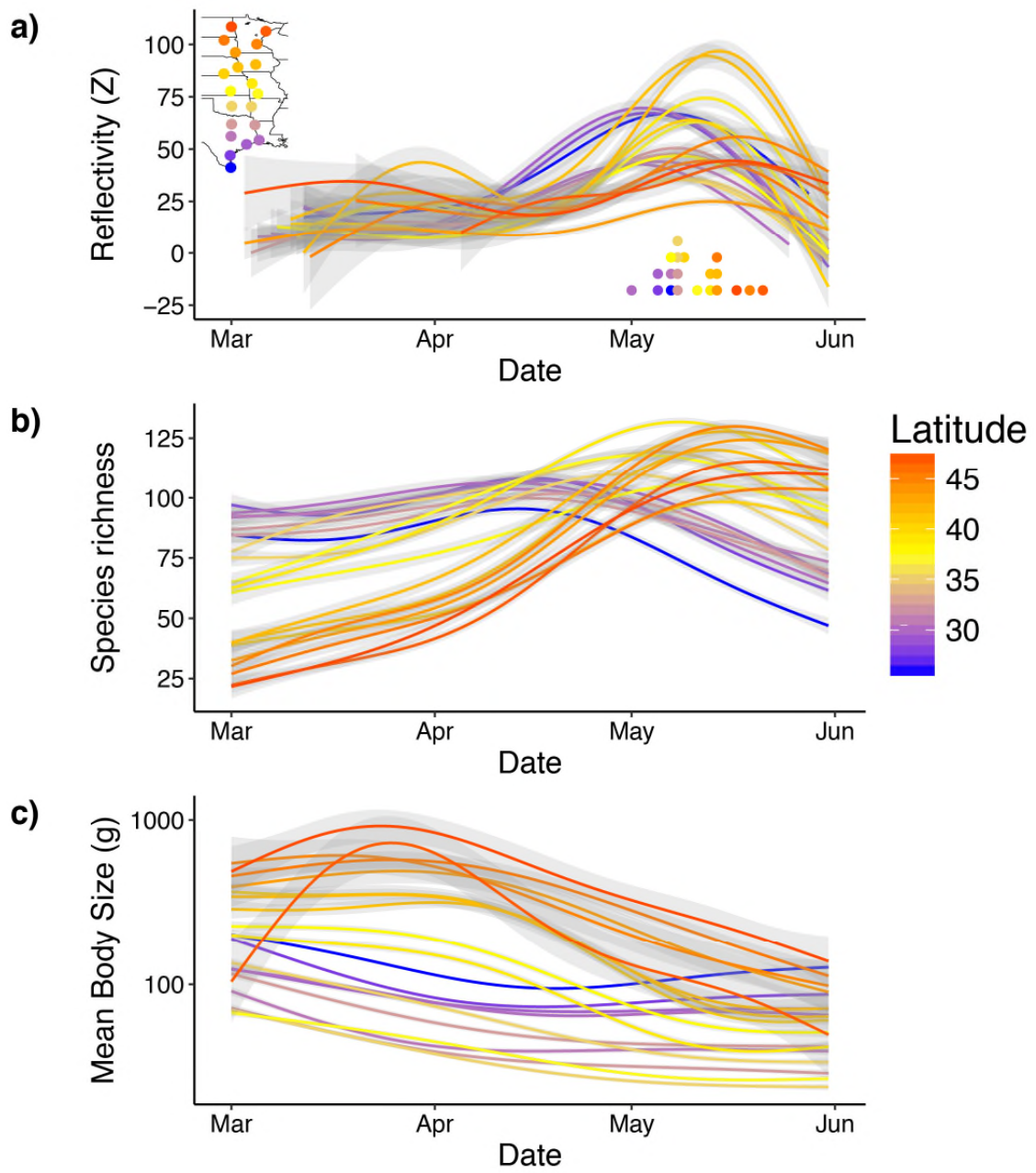


Figure 2:

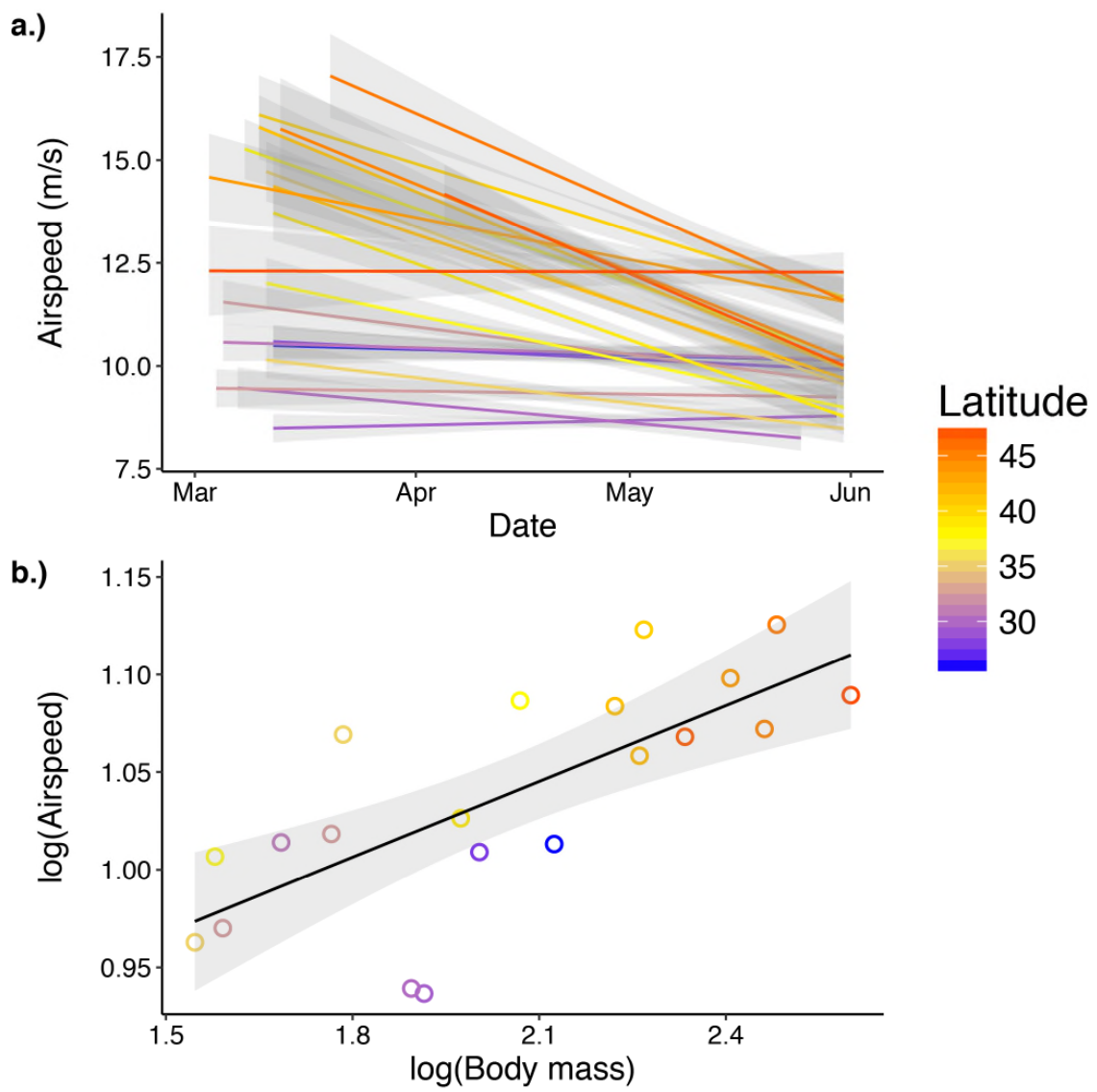


Figure 3:

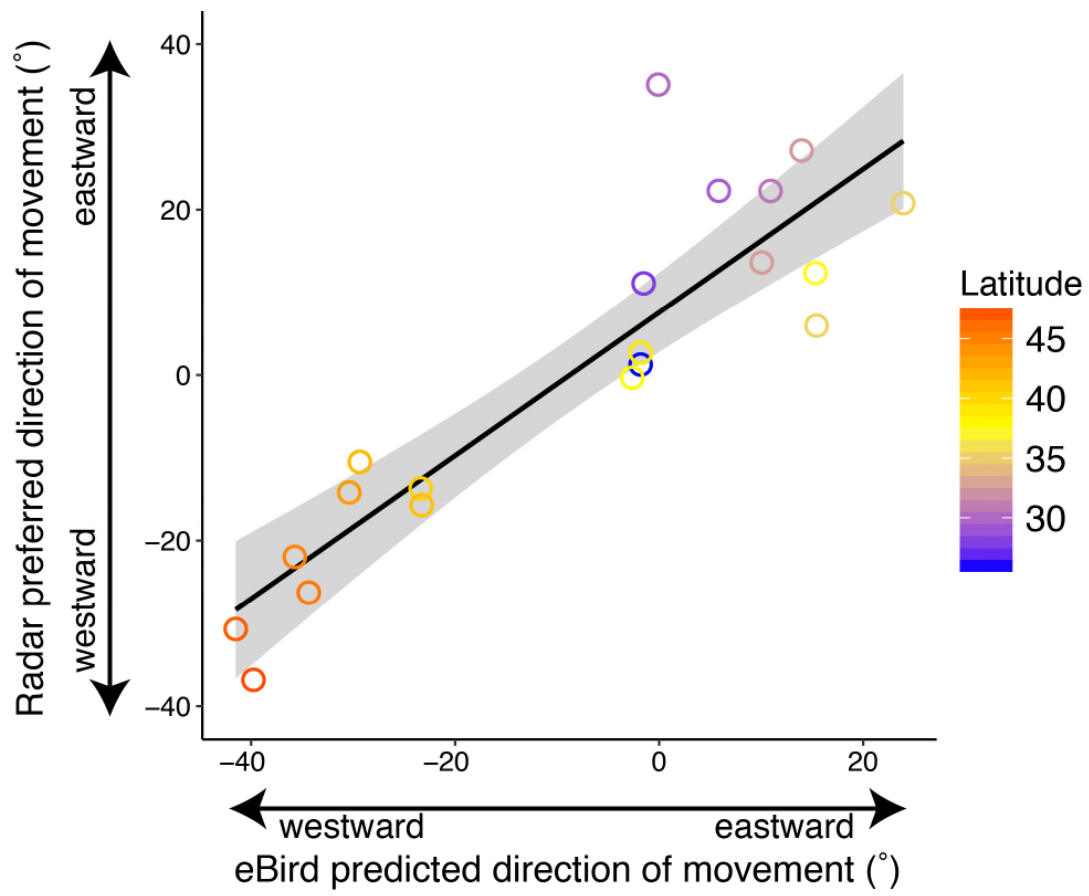


Figure 4:

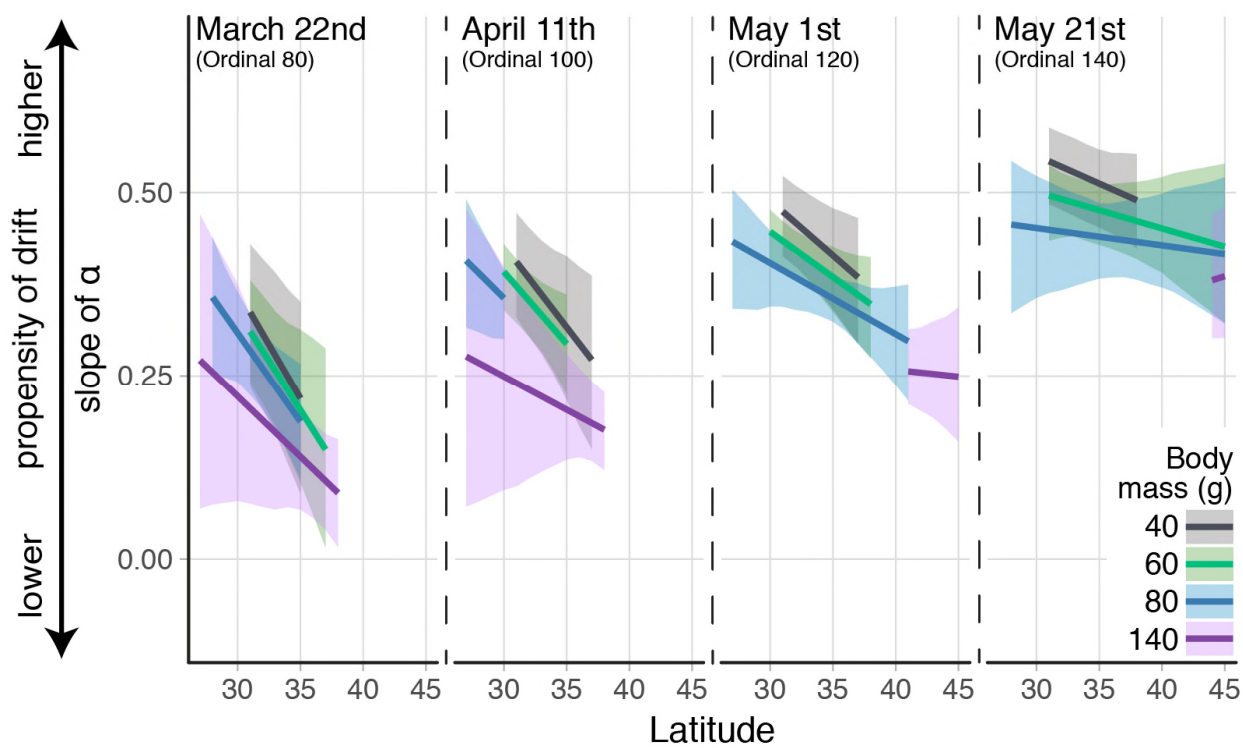


Figure 5:

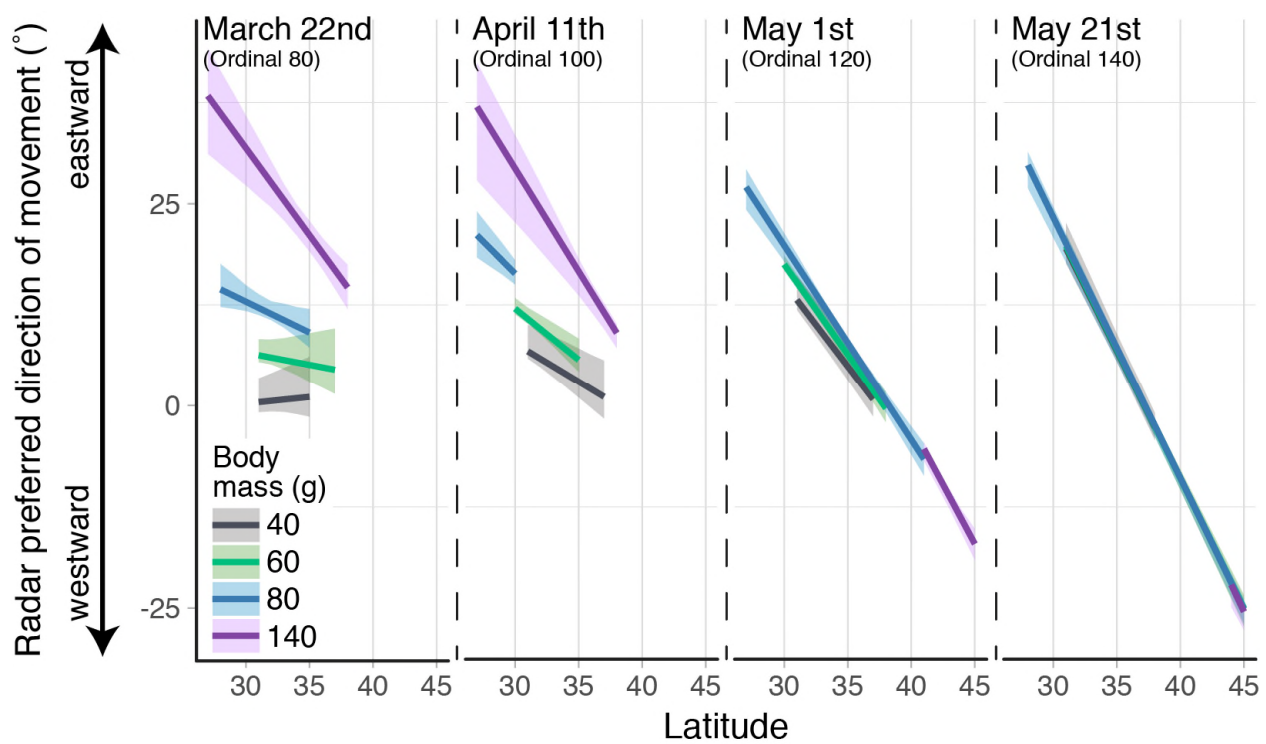


Figure 6:

Figure legends:

Figure 1: Rose diagram showing the distribution of migrant track (pink) and heading (blue) during spring migration (2013-15) from 20 weather surveillance radar (WSR) stations locations in the central USA. Black arrows identify the modeled in-flight preferred direction of movement. We weighted track and heading distributions by scaled reflectivity factor and used 20° sectors for the plotting of track and heading measures. The color of the WSR stations is based on its latitude.

Figure 2: Bird migration characterizations by time and latitude in the central USA. (a) Reflectivity as measured by 20 weather surveillance radar (WSR) stations during spring migration (2013-15). The fitted lines and 95% confidence bands are from generalized additive models. The colored points are the estimated peak migration date (highest modeled reflectivity) for each WSR station. Points depicted in multiple rows because of overlapping date. (b) Weekly species richness and (c) log-scaled mean body size of migrating birds based on STEM estimates of probability of occurrence using bird observations from eBird.

Figure 3: (a) Airspeeds of migrants measured at 20 weather surveillance radar (WSR) stations during spring migration (2013-15). The fitted lines and 95% confidence bands are from least squares linear models. (b) Log-transformed migrant airspeed (m/s) and averaged body mass (g). The fitted line and 95% confidence band is from least squares linear models ($R^2=0.54$). Only airspeeds with

northward track directions were considered ($< 90^\circ$ and $> 270^\circ$). The scaling relationship is described as follows: $\text{airspeed} = 5.93 \times (\text{mass})^{0.13}$. WSR station color corresponds to its latitude.

Figure 4: Radar preferred direction of movement and eBird predicted direction of movement during spring migratory periods (2013-15) at 20 weather surveillance radar (WSR) stations. Fitted line and 95% confidence band estimate associations ($R^2=0.84$). WSR station color corresponds to its latitude.

Figure 5: Wind drift propensity across latitudes at 20 weather surveillance radar stations during spring migration (2013-15). Slope of α represents drift propensity; 0 is complete compensation for wind, 1 is complete drift with wind. Predictions of propensity of drift are shown at 20 day intervals (80, 100, 120, and 140) for the 20th, 40th, 60th, and 80th percentiles of body mass (grams). The fitted lines and 95% confidence bands are from a mixed-effects model (see methods for details). Predictions only plotted for ranges for which behavioral observations were represented in our dataset.

Figure 6: Radar preferred direction of movement across latitudes at 20 weather surveillance radar stations during spring migration (2013-15). Predictions of preferred direction of movement are shown at 20 day intervals (80, 100, 120, and 140) for the 20th, 40th, 60th, and 80th percentiles of body mass (grams). The fitted lines and 95% confidence bands are from a mixed-effects model (see methods for

details). Predictions only plotted for ranges for which behavioral observations were represented in our dataset.